



Cite this: *Sens. Diagn.*, 2023, 2, 480

Received 27th December 2022,
Accepted 10th February 2023

DOI: 10.1039/d2sd00232a

rsc.li/sensors

Electrochemiluminescence devices for point-of-care testing

Xudong Ying, Lin Zhou, Wenxuan Fu, Yafeng Wang and Bin Su  *

Point-of-care testing (POCT) is also known as near-patient or on-site testing. Because of its speediness, high efficiency, low cost, and excellent convenience, POCT has been widely used in clinical diagnosis, infectious disease surveillance, drug screening, and food quality monitoring. Electrochemiluminescence (ECL) is a powerful transduction technique in biosensing and immunodiagnostics, thus attracting more and more research attention in POCT applications. In this article, we present an overview of various ECL-POCT devices that have been developed so far. The article will begin with a short introduction of different types of ECL-POCT devices. Then we shall discuss the categories, detection strategies, and application scenarios of current ECL-POCT devices. The article finally ends up with a short conclusion and perspectives. We hope this article is helpful for understanding, constructing, and designing ECL devices for POCT.

1. Introduction

Point-of-care testing (POCT) is a method for real-time analysis of patient specimens outside the laboratory, near or at the site of the patient.¹ Thanks to its speediness, high efficiency, low cost, excellent convenience, and low operation requirements, POCT has been widely used in clinical diagnosis, infectious disease surveillance, drug screening, food security, and many other fields.^{2–4} POCT devices are highly desirable in the global market, especially for *in vitro* diagnostics (IVD). They play a very important role in improving patient safety and diagnostic efficiency, in particular during a pandemic such as COVID-19 and H1N1

Key Laboratory of Excited-State Materials of Zhejiang Province, Institute of Analytical Chemistry, Department of Chemistry, Zhejiang University, Hangzhou 310058, China. E-mail: subin@zju.edu.cn

influenza.^{5–10} As reported recently, the global POCT market was about 35.5 billion dollars in 2021 and is expected to exceed 96.0 billion dollars in 2025.¹¹

POCT devices can report the detection results by different methods, such as electrochemistry (EC), high-performance liquid chromatography (HPLC), electrochemiluminescence (ECL), fluorescence (FL), etc.^{12–15} Among them, ECL is an ideal one for POCT, because of its advantages of high sensitivity, low background, no requirement of an external light source for excitation and high spatiotemporal controllability.^{16,17} Therefore, in the last decade, a variety of ECL-POCT devices have been developed, including microfluidic paper-based analytical devices (μPADs), lateral flow strips (LFS), and ECL cells (as summarized in Fig. 1), and widely used in public or personal health caring and disease diagnosis. Although numerous studies have been



Xudong Ying

Xudong Ying received his B.S. degree in 2021 at Hangzhou Normal University. Now he is a Master student at Zhejiang University. His research interests are focused on electrochemical methods for lateral flow bioassays.



Lin Zhou

*Lin Zhou received his B.S. degree in 2017 at Zhejiang Sci-Tech University and PhD. degree in 2022 at Zhejiang University. His current research interests are in the fields of *in vivo* bioanalysis and electrochemical biosensors.*



carried out to improve the sensitivity and integration of ECL-POCT devices, it is still challenging to achieve full portability, de-laboratory, de-specialization, and automation.

This review aims to discuss various ECL-POCT devices and their applications. We shall first present the mechanism of ECL and the detection strategies commonly used in ECL-POCT devices. Subsequently, we classify and briefly introduce ECL-POCT devices and discuss in detail the performance of ECL-POCT devices in different application scenarios. The article will end with a short conclusion and perspectives.

2. The testing strategy for ECL-POCT

The ECL process is very complicated, which involves not only heterogeneous electrochemical reactions but also homogeneous chemical reactions between electrogenerated intermediates. Understanding the mechanism of ECL



Wenxuan Fu

Wenxuan Fu received his B.S. degree from Northwest University in 2020. Now he is a PhD student at Zhejiang University. His research interests are focused on electrochemical lateral flow bioassays and electrochemiluminescence sensors.



Yafeng Wang

Yafeng Wang received his B.S. degree from the Zhejiang University of Technology in 2014 and Ph.D. degree from Zhejiang University in 2020. He is now a postdoctoral fellow at Zhejiang University. His research interests are focused on electrochemiluminescence, spatiotemporal electrochemistry and immunoassays.

generation is essential to the design and fabrication of high-performance ECL-POCT devices. On the other hand, the testing strategies of ECL-POCT are also very important for constructing efficient devices and should be adjusted elaborately according to the target species.

2.1 The mechanism of ECL

Generally, ECL can be produced by either the annihilation or the coreactant pathway.²⁴ In the former, the radical anion and cation are electrogenerated on the cathode and anode, respectively, which then react with each other to generate excited state species. The excited state species relax to the ground state and emit light. Meanwhile, in the coreactant pathway, a positive or negative unidirectional step potential or potential scan is applied on the working electrode to electrochemically oxidize or reduce the luminophore and coreactant. The electrogenerated intermediates undergo homogeneous electron-transfer reactions to form the excited state luminophore, followed by light emission through relaxation of the excited state luminophore to the ground state. Luminophores play an important role in ECL reactions. Ruthenium(II) complexes, luminol, and quantum dots (QDs) are frequently used in most previous studies.^{25,26}

2.2 Sensing strategies of ECL-POCT

Analytes can be generally divided into ions, small molecules, nucleic acids, proteins, and cells.²⁷ Different testing strategies can be adopted depending on the nature of analytes.

Nucleic acids, proteins, and cells are usually analyzed by sandwich assays because they have specific sites for recognition and functionalization. Sandwich assays typically require simultaneous binding of recognition and signaling probes. As shown in Fig. 2A, the most important step of the



Bin Su

Bin Su received his B.I. degree from Jilin University, M.S. from the Chinese Academy of Sciences and Ph.D. from Ecole Polytechnique Fédérale de Lausanne (EPFL). After three years of postdoctoral research at EPFL, he started his independent research at Zhejiang University in 2009. He has served as the Director of the Institute of Analytical Chemistry at Zhejiang University since 2016 and was promoted to Qiushi Distinguished

*Professor in 2022. His research interests cover analytical chemistry and electrochemistry, including interfacial electrochemistry, electrochemical biosensors *in vivo* and brain electroanalysis. He has authored more than 180 peer-reviewed journal papers and 3 book chapters, and also holds 11 Chinese patents.*



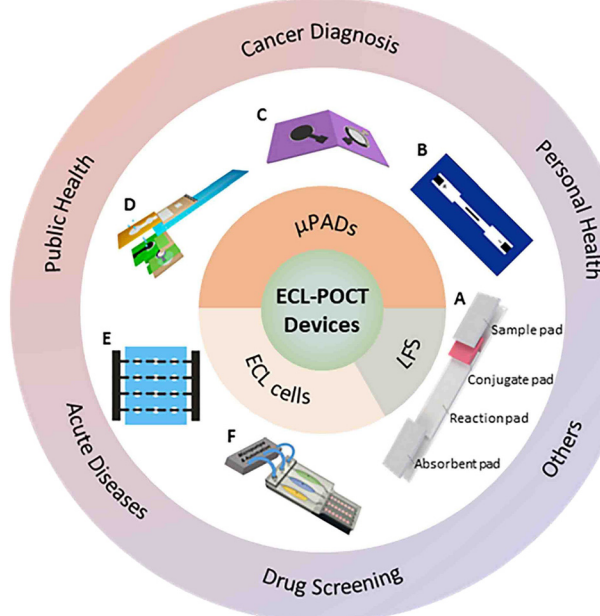


Fig. 1 Schematic summary of the main types of ECL-POCT devices and their applications. The lateral flow strip (LFS, A)¹⁸ (Copyright 2020, Springer Nature). Microfluidic paper analytical devices (μ PADs) including those based on an open bipolar electrode (B),¹⁹ (Copyright 2015, Elsevier), folding paper (C)²⁰ (Copyright 2013, Elsevier) and a dual-mode lab-on-paper platform (D)²¹ (Copyright 2020, American Chemical Society). The full-featured ECL sensing platform based on a multichannel closed bipolar system (E)²² (Copyright 2014, American Chemical Society) and a three-dimensional (3D) printed microfluidic array (F)²³ (Copyright 2017, American Chemical Society).

assay is to sandwich the analyte between recognition molecule 1 and recognition molecule 2 labeled with a signaling marker.²⁷ Typically, the analyte and the labeled recognition molecule 2 are pre-incubated for a period of time to form a conjugated compound, which is then added to the substrate immobilized with recognition molecule 1 to form a

sandwich structure. ECL probes and enzymes are the most commonly used signaling markers. Since ECL intensity is proportional to the amount of ECL probe or enzyme, the concentration of analytes can be determined. In addition to the sandwich assay, hairpin nucleic acid structures and specific cleaving enzymes can also be used in nucleic acid-based analysis.

ECL probes or enzymes are usually needed for the detection of small molecules and ions. Small molecular species can be directly or indirectly involved in ECL reactions and the relationship between their concentrations and changes of ECL intensity can be established to accomplish trace analysis. For example, NH_3 and H_2O_2 can be directly used as coreactants for ECL reactions.^{28,29} Dopamine (DA) can function as a coreactant and can also quench the ECL signal of $\text{Ru}(\text{bpy})_3^{2+}$.^{30,31} Pb^{2+} can drive specific DNA enzymes to cut certain nucleic acid chains.²¹ Glucose can produce specific molecules under the catalysis of oxidase or dehydrogenase to participate in ECL reactions.^{32,33} Thus, DA, Pb^{2+} , and glucose can all be indirectly determined by ECL.

3. ECL-POCT devices

ECL-POCT devices basically can be classified into three types: LFS, μ PADs, and ECL cells (Fig. 1).^{11,16,34} Both LFS and μ PADs possess the ability to separate complex samples through the capillary action of cellulose materials, but LFS have a specific structure for sample addition, target recognition and capture. ECL cells can emit light steadily for a long time, thus avoiding the instability caused by solution evaporation. In this section, we briefly describe these three types of devices.

3.1 LFS

The LFS, as the most widely used sensor in POCT devices, has been employed in detecting a variety of target substances in different bio-samples, including serum, blood, food, etc.¹⁸ The operation of the LFS relies on the capillary flow of the sample in a series of paper pads. The standard LFS consists of a sample pad where the sample is dropped, a conjugate pad with labeled biorecognition elements, a reaction membrane where target DNA-probe DNA hybridization or antigen-antibody interaction occurs on the test line and control line, and finally an absorbent pad that reserves the waste (Fig. 2B).³⁵ Each pad is designed purposely to produce a signal indicating the absence/presence or concentration of the analyte of interest. The gold nanoparticle-based LFS is the most widely used one, which, however, in most cases only allows qualitative analysis.¹⁸ Different from traditional LFS, ECL-based LFS need electrodes and solutions for reaction, as well as specific devices for ECL signal excitation and readout. ECL-based LFS have significant advantages over other optical detection methods due to their versatility and simplified optical setup for light generation and detection.³⁶ They indeed have shown a high sensitivity and wide detection range for quantitative analysis.³⁷⁻³⁹

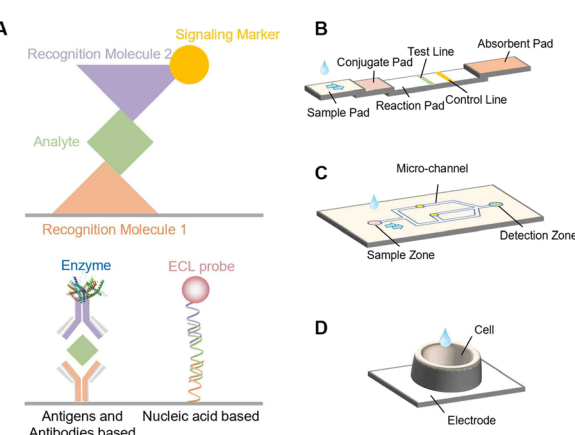


Fig. 2 (A) Scheme of sandwich assays. (B) Schematic diagram of a typical structure of LFS. (C) Schematic diagram of a typical structure of μ PADs. (D) Schematic diagram of a typical structure of ECL cells.



3.2 μ PAD

A μ PAD is a kind of microfluidic device that uses cellulose or fiber as the substrate that can transport fluid from an inlet through a porous medium to a desired outlet or region of the device by means of capillary action.⁴⁰ Through various processing technologies, hydrophilic/hydrophobic micro-channel networks and related analysis devices have been designed to construct “lab on paper”. In comparison with LFS, no specific patterns or regulations for μ PAD construction are needed (Fig. 2C). ECL-based μ PADs have several advantages, including low cost, high flexibility, and ease of analyte immobilization.^{41,42} In addition, the generation of ECL signals can be also potentially- and spatially controlled.⁴³ Therefore, ECL-based μ PADs have received increasing attention in biomedical analysis, clinical diagnosis, food processing, *etc.* In particular, the combination of μ PADs with screen-printed electrodes further expands the detection range and shows a good prospect for the detection of trace analytes.⁴³

3.3 ECL cells

An ECL cell refers to a kind of device that has a specific area for solution holding. Different from the other two types of devices, ECL cells do not use paper as a carrier for holding the solution. The cells are usually made by 3D printing technology and can hold adjustable volumes of samples.^{23,44} This kind of device can secure the effective use and stability of the electrode and allow long-time stable ECL analysis. In addition, they can be readily used for array analysis (Fig. 2D). However, the sensitivity, selectivity and antifouling performance of used electrodes must be improved for the analysis of complex samples, such as interstitial fluid, serum and blood.

4. Applications of ECL-POCT devices

In recent years, ECL-POCT devices have been widely used in various fields, such as clinical diagnosis, infectious disease surveillance, drug screening and food quality monitoring (Table 1). These devices have advantages of high sensitivity, high selectivity, rapid detection, and analysis of complex matrices without extensive pretreatment.^{16,34} In practical analysis, ECL-POCT devices can solve the problem of real-time detection of low concentration markers and the dilemma of timely judgment. In this section, the applications of ECL-POCT devices are summarized.

4.1 Cancer diagnosis

Nowadays, cancer-related markers can be successfully detected by ECL-POCT devices. Three-dimensional paper microfluidic devices have complex fluid networks and detection zones for POCT. The Yu group⁴⁷ proposed a 3D μ PAD ECL device for detecting multiple cancer markers in human serum (Fig. 3A). This device can distribute samples from a single-entry point to multiple detection areas to avoid

interference of ECL signals from adjacent working electrodes. Later, the group reported a series of 3D μ PAD ECL devices to detect cancer markers in human serum with better assay performance.^{69–71} For example, as shown in Fig. 3B, they fabricated a 3D μ PAD ECL immunosensor for CEA using a nanoporous gold-chitosan-modified paper working electrode (NGC-PWE) and graphene QD (GQD) functionalized Au-Pt NPs.⁴⁸ These studies integrated the paper electrode with the support, so that the device could achieve good electrical contact. But the process of fabricating this type of device is time-consuming. The devices are usually prepared *via* a layer-by-layer assembly strategy, which is not suitable for large-scale production. To overcome this limitation, the group later developed a series of 3D folded μ PADs for the detection of cancer makers,^{72–74} which are more integrated than their previous versions.

Cancer cell detection is an important component and basis of cancer diagnosis and treatment.²⁵ Yu *et al.*⁴⁹ developed an origami microfluidic device as an efficient platform for cancer cell detection, in which an aptamer modified 3D microporous Au-paper electrode was used as the working electrode (Fig. 3C). The limit of detection can reach 250 cells per mL. The same sandwich immunoassay mode and different probes were then used in other works.^{75,76} The detection limit is as low as 40 cells per mL. In addition, the activity of cancer cells can also be studied by measuring the level of relevant molecules, such as adenosine triphosphate (ATP)⁷⁷ and H_2S .⁷⁸

Innovation of the testing strategy can effectively improve the sensitivity of detection. As shown in Fig. 3D, Wang *et al.*⁴⁵ developed an ECL-POCT device based on a constant resistance closed bipolar electrode for detecting a prostate cancer marker, namely, miRNA-141, allowing the readout by the naked eye. The device consists of an indium tin oxide (ITO) glass with screen-printed bipolar electrodes for ECL detection and polydimethylsiloxane (PDMS) with a specific channel structure for sample pre-treatment. This device provides a two-color analysis mode, which can improve not only the resolution of visual observation but also the sensitivity through ratio analysis of the ECL intensity. Song *et al.*⁴⁶ reported a self-reinforcing solid-state ECL system for *in situ* detection of the activity of caspase-3 (Fig. 3E). In this system, the analyte was used as a switch for ECL signaling. A peptide chain with ferrocene (Fc) was then introduced, which could be specifically cleaved by caspase-3. After the digestion reaction, the ECL intensity increased due to the departure of the Fc quenching group. This strategy can greatly reduce the steps and time required for biomarker detection, in good consistency with the concept of POCT. In addition, the detection limit of this solid-state ECL system for caspase-3 is as low as 0.017 pg mL^{-1} , due to the fixation of ECL probes on the electrode surface.

4.2 Public health surveillance

Public health sustains the security of a nation and covers the extensive control of infectious diseases, environmental pollution, food safety, and many other perspectives.



Table 1 Summary of ECL-POCT devices with their analytic performance

Application	Device	Categories	Analyte	Limit of detection	ECL system	Ref.
Cancer diagnosis	“Color switch” ECL ratiometric biosensor	ECL cell	miRNA-141	10^{-17} mol L ⁻¹	$\text{Ru}(\text{bpy})_3^{2+}/\text{TPrA}$ & BNQD/ $\text{S}_2\text{O}_8^{2-}$	45
	Self-enhanced ECL biosensor	ECL cell	Caspase-3	0.017 pg mL ⁻¹	$\text{Ru}(\text{dcbpy})_3^{2+}/\text{PEI}$	46
	3D paper-based ECL device	μPAD	AFP	0.15 ng mL ⁻¹	$\text{Ru}(\text{bpy})_3^{2+}/\text{TPrA}$	47
			CA125	0.6 U mL ⁻¹		
			CA19-9	0.17 U mL ⁻¹		
			CEA	0.5 ng mL ⁻¹		
	Supercapacitor-powered ECL protein immunoarray	ECL cell	PSA	0.3 pg mL ⁻¹	$\text{Ru}(\text{bpy})_3^{2+}/\text{TPrA}$	44
			PSMA	0.535 pg mL ⁻¹		
Public health			PF-4	0.42 pg mL ⁻¹		
	3D origami device	μPAD	CEA	0.6 pg mL ⁻¹	$\text{GQDs}/\text{H}_2\text{O}_2$	48
	Microfluidic paper-based ECL origami cyto-device	μPAD	MCF-7	250 cells per mL	$\text{O}_2/\text{S}_2\text{O}_8^{2-}$	49
	pBPE-ECL molecular switch system	μPAD	<i>Listeria monocytogenes</i>	10 copies per μL	$[\text{Ru}(\text{phen})_2\text{dppz}]^{2+}/\text{TPrA}$	50
	Microfluidic paper electrochemical device	μPAD	Benzo[a]pyrene	150 nmol L ⁻¹	Ru-PVP/guanines	51
	PCR-free ECL sensor	ECL cell	HBV	0.05 cps μL^{-1}	$[\text{Ru}(\text{phen})_2\text{dppz}]^{2+}/\text{S}_2\text{O}_8^{2-}$	52
	Biosensor combining immunoliposome and ECL	ECL cell	H1N1	2.7×10^2 to 2.7×10^3 PFU mL ⁻¹ (detection range)	$\text{Ru}(\text{bpy})_3^{2+}/\text{triethyl-amine}$	53
	Smartphone-based ECL system	ECL cell	<i>E. coli</i>	5 cfu mL ⁻¹	$\text{Ru}(\text{bpy})_3^{2+}/\text{TPrA}$	54
Personal health	Visual and ratiometric ECL dual-readout assay device	μPAD	Pb ²⁺	3 pmol L ⁻¹	Luminol/ H_2O_2 & CdS	21
	Closed BPE-based ECL devices	ECL cell	Choline	1.25 $\mu\text{mol L}^{-1}$	QDs/ H_2O_2	
			Dopamine	0.33 $\mu\text{mol L}^{-1}$	$\text{Ru}(\text{bpy})_3^{2+}/\text{TPrA}$ & Luminol/ H_2O_2	55
	3D-printed portable system	ECL cell	Vitamin B ₁₂	0.107 nmol L ⁻¹ & 0.094 nmol L ⁻¹	Luminol/ H_2O_2	56
	64-Microwell ECL array	ECL cell	8-oxodG	0.15%	Os-complexes/8-oxoguanine	57
	Dual enzymatic sensor	ECL cell	Glucose	25 $\mu\text{mol L}^{-1}$	$[\text{Ru}(\text{bpy})_3]^{2+}/\text{NADH}$	33
			Choline	50 $\mu\text{mol L}^{-1}$	Luminol/ H_2O_2	
	Single-electrode ECL system	ECL cell	H_2O_2	0.27 $\mu\text{mol L}^{-1}$	Luminol/ H_2O_2	58
Acute diseases	Smartphone based ECL analysis device	ECL cell	Glucose	—		
			Uric acid	—		
	Paper-based bipolar ECL biosensor	μPAD	3-Nitrotyrosine	8.4 nmol L ⁻¹	$\text{Ru}(\text{dcpb})_3^{2+}/\text{TPrA}$	59
	Lateral flow immunosensor	LFS	Choline	0.573 $\mu\text{mol L}^{-1}$	Luminol/ H_2O_2	60
			Lactate	3.132 $\mu\text{mol L}^{-1}$		
	Dry chemistry-based ultrasensitive ECL immunosensor	LFS	Cholesterol	7.418 $\mu\text{mol L}^{-1}$	$\text{Ru}(\text{bpy})_3^{2+}/\text{L-Cys}$	37, 38
			cTnI	0.81 pg mL ⁻¹		39
	Raspberry Pi-based ECL biosensor	ECL cell	CRP	4.6 pg mL ⁻¹		
Drugs screening	Carbon ink SEES	ECL cell	cTnI	0.4416 pg mL ⁻¹	$\text{Ru}(\text{bpy})_3^{2+}/\text{L-Cys}$	61
	ECL molecularly imprinted polymer (ECL-MIP) sensor	ECL cell	Nitrofurazone	0.09 nmol L ⁻¹	Luminol/ H_2O_2	62
	ECL sensing platform based on deep learning-assisted smartphone strategy	ECL cell	Furosemide	0.25 $\mu\text{mol L}^{-1}$	$\text{CsPbBr}_3/\text{S}_2\text{O}_8^{2-}$	63
	Smartphone-based ECL system	ECL cell	Nitroaromatic explosives	2.3 pg mL ⁻¹	CdS QDs/ $\text{S}_2\text{O}_8^{2-}$	64
Explosives	Portable ECL sensor based on SPE	ECL cell	Abolin	5 pg mL ⁻¹	$\text{Ru}(\text{bpy})_3^{2+}/\text{TPrA}$	65
	Paper-based bipolar electrode ECL sensor	μPAD	$\text{A}\beta(1-42)$	100 pmol L ⁻¹	$[\text{Ru}(\text{phen})_2\text{dppz}]^{2+}/\text{TPrA}$	66
	ECL based aptasensor	ECL cell	β -Lactoglobulin	1.36 $\mu\text{g L}^{-1}$	Luminol/ H_2O_2	67

bpy = bipyridine, BNQD = boron nitride quantum dots, dcby/dcpb = 4,4'-dicarboxyl-2,2'-bipyridine, PEI = polyethyleneimine, AFP = alpha fetoprotein, CA = cancer antigen, CEA = carcinoembryonic antigen, PSA = prostate specific antigen, PSMA = prostate specific membrane antigen, PF = platelet factor, MCF-7 = human breast cancer cell line, phen = 1,10-phenanthroline, dppz = dipyrro[3,2-*a*:2',3'-*c*]phenazine, PVP = polyvinyl pyrrolidone, HBV = hepatitis B virus, 8-oxodG = 8-oxo-7,8-dihydro-2'-deoxyguanosine, NADH = nicotinamide adenine dinucleotide, cTnI = cardiac troponin I, L-Cys = L-cysteine, SEES = single-electrode electrochemical system, SPE = screen-printed electrode.



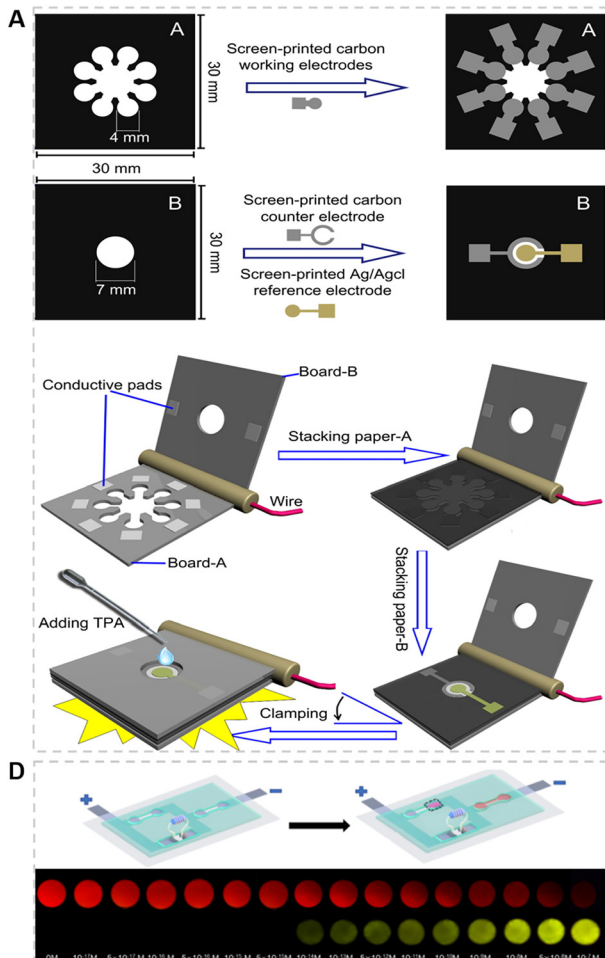
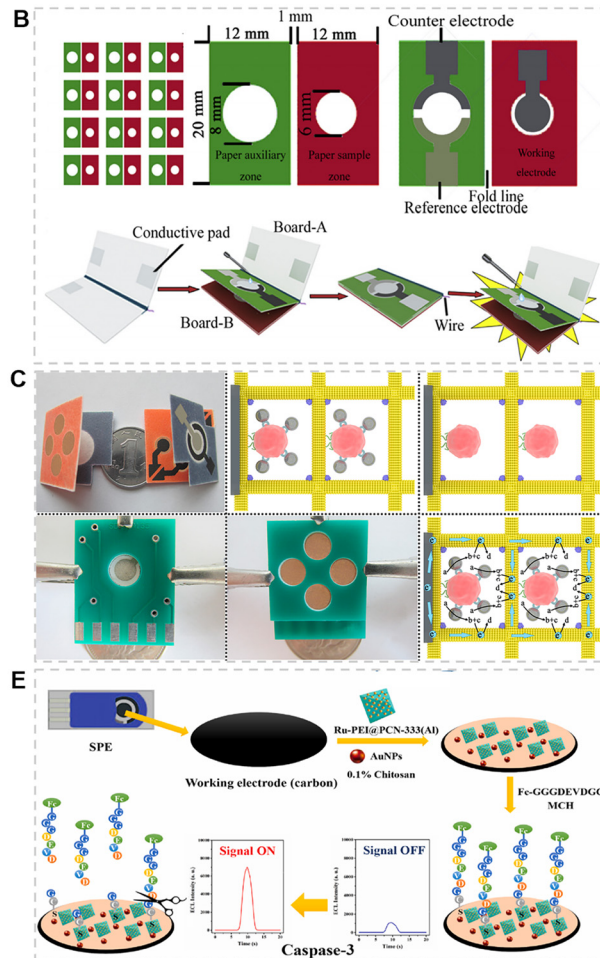


Fig. 3 (A) The procedure for fabricating a simple homemade 3D paper-based ECL device. Paper sheets were firstly patterned using a wax printer, then electrodes were screen-printed on sheet-A and sheet-B, respectively. Finally, sheet A and sheet B were cut into paper A and paper B with the same size ($30.0\text{ mm} \times 30.0\text{ mm}$).⁴⁷ Copyright 2012, Elsevier. (B) Schematic illustration of the size, shape, and detection of a 3D origami ECL device.⁴⁸ Copyright 2014, Elsevier. (C) The fabrication and operation procedures of an origami microfluidic device.⁴⁹ Copyright 2015, Elsevier. (D) Structure and sensing result of the naked eye direct-reading ECL platform.⁴⁵ Copyright 2022, American Chemical Society. (E) Sensing diagram of the self-reinforcing solid-state ECL system.⁴⁶ Copyright 2022, Elsevier.



Infectious diseases are caused by pathogens such as fungi, bacteria, viruses and parasites. Viral infectious diseases are the most concerning, which are characterized by adaptability and rapid mutation, so that rapid screening and halting transmission are crucial. Recently, numerous ECL-POCT devices have been developed to detect viruses.^{52,53,79-81} For antigen detection, Egashira *et al.*⁵³ reported an ECL based immunosensor for the detection of H1N1 (Fig. 4A), in which an Au electrode modified with a hemagglutinin (HA) peptide was used as the working electrode. The HA peptide can compete with the H1N1 virus to bind with $\text{Ru}(\text{bpy})_3^{2+}$ -encapsulated immunoliposomes. When the concentration of the virus is low, more liposomes will be trapped on the electrode surface. After cleaning and pre-treating the electrode, $\text{Ru}(\text{bpy})_3^{2+}$ is released to generate a high ECL intensity. For nucleic acid detection, Conoci *et al.*⁵² developed a PCR-free ECL device to detect a synthetic HBV genome in real samples. As shown in Fig. 4B, two probes were employed to anchor the HBV gene simultaneously. The HBV genome

can be detected by signal amplification of $[\text{Ru}(\text{phen})_2\text{dppz}]^{2+}$. The limit of detection was $0.06\text{ cps } \mu\text{L}^{-1}$. The two aforementioned methods significantly improve the detection sensitivity through the strategy of signal amplification. Moreover, the latter introduces two probes and exhibits a higher selectivity to the virus, but it requires a long analysis time and is not conducive to the immediate detection of the virus.

With global industrialization, sewage pollution has been a serious environmental problem. Some chemicals such as ammonia and heavy metals are of particular concern. For ammonia detection, Tamer *et al.*²⁸ reported an ECL gas sensor to detect the total ammonia concentration in water samples (Fig. 4C). The device was fabricated by 3D printing and integrated with a paper electrode and an optical fiber. After heating the sample, NH_3 in the sample can be transferred to the paper electrode and participate in ECL reaction as a coreactant to realize the detection. The method is also suitable for environmental and

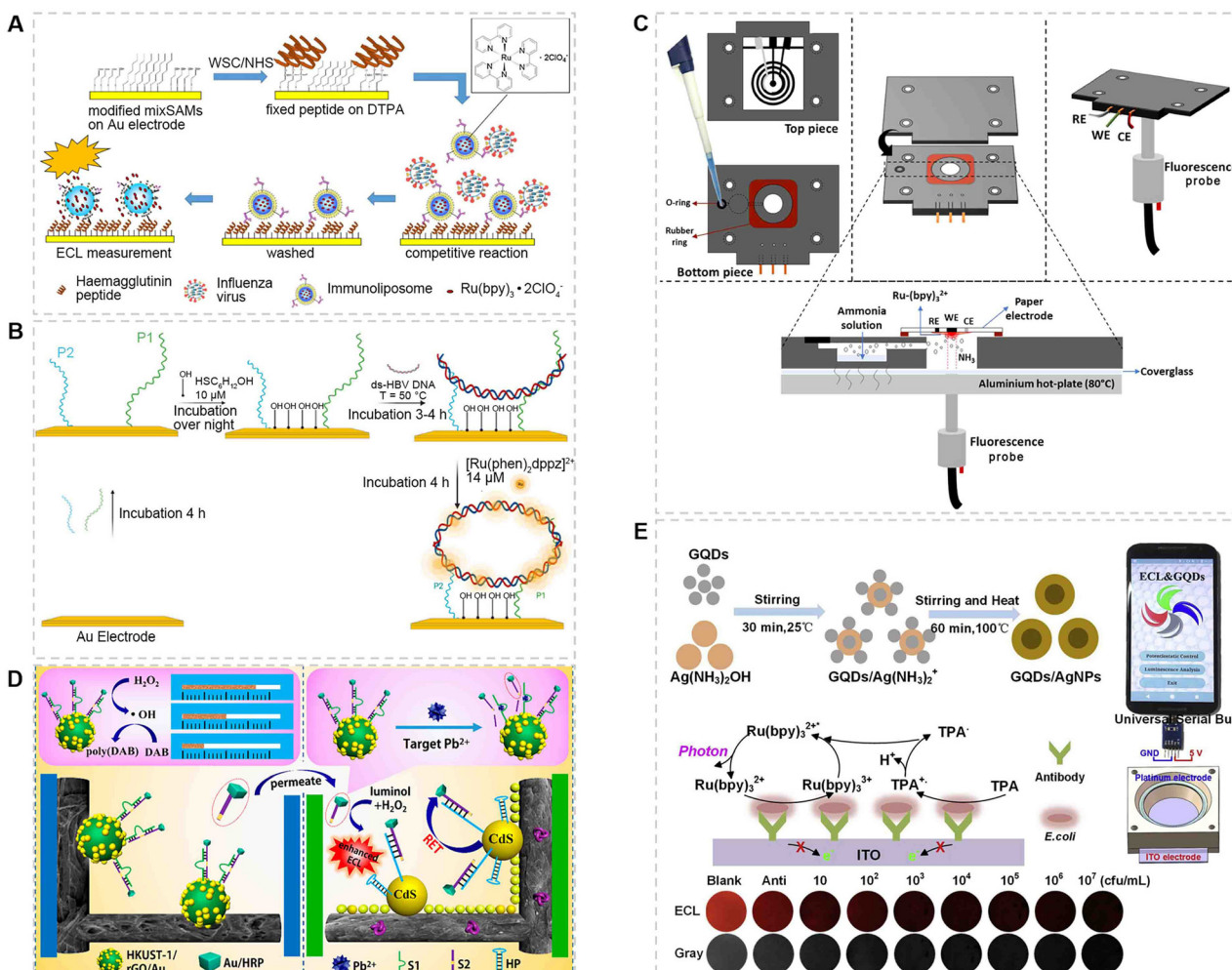


Fig. 4 (A) ECL immunosensor based on a hemagglutinin modified gold electrode for the detection of the H1N1 virus.⁵³ Copyright 2016, Springer Berlin Heidelberg. (B) Schematic illustration of the ECL-PCR-free strategy using two probes for the detection of the HBV genome.⁵² Copyright 2022, Elsevier. (C) 3D printed ECL device with a paper electrode and pre-heating treatment for the detection of NH₃ in water samples.²⁸ Copyright 2022, Elsevier. (D) The distance-based visual semiquantitative analysis and ratiometric ECL accurate assay of Pb²⁺ in water samples.²¹ Copyright 2020, American Chemical Society. (E) Preparation of GQD/AgNP nanocomposites as ECL signal amplification reagents on an ITO electrode for the detection of *E. coli* using a smartphone-based system.⁵⁴ Copyright 2019, Elsevier.

biological samples.⁸² For heavy metal detection, Yu *et al.*²¹ developed a POCT device allowing visual readout and ECL ratio analysis of Pb²⁺ in water samples (Fig. 4D). Although the sensitivity of this ECL-POCT device can be further improved, its quantitative and equipment-free testing capability is very suitable for non-specialists.⁸³

Another threat in sewage is pathogenic bacteria, such as *Escherichia coli* (*E. coli*) and *Clostridium perfringens*.^{54,84} *E. coli* is used as a stool indicator to evaluate water quality, since an excessive amount of *E. coli* will cause the deterioration of water.⁸⁵ Although most types of *E. coli* are beneficial, some are dangerous and even fatal, such as *E. coli* O157:H7.^{85,86} The Liu group⁵⁴ has designed a smartphone-based ECL system for the detection of *E. coli*, in which GQD/AgNP nanocomposites were modified on the ITO surface to amplify and stabilize the ECL signal (Fig. 4E). The luminescence images could also be

processed using a smartphone. Eventually, a wide linear range and a low limit of detection to *E. coli* were obtained. In this work, a simple device coupled with smartphone data analysis better demonstrated the advantages of POCT devices.

Few articles regarding food safety have been reported, and tests for the preservative H₂O₂ (ref. 87 and 88) and a bacterium, *Listeria monocytogenes*,⁵⁰ have been performed. H₂O₂, as a commonly used preservative, will pose a threat to human health if being added excessively. *Listeria* is a foodborne pathogen that causes abortion, sepsis and meningitis in animals and humans.^{89,90} It can still survive and reproduce at 4 °C and is one of the main pathogens threatening human health in refrigerated food. Therefore, testing *Listeria* in refrigerators is especially important. For this purpose, ECL-POCT devices have an absolute advantage.

4.3 Detection of physiological signs

There are many small molecules in the human body that maintain normal physiological activities. High or low levels of them can lead to abnormal changes in the body. Some molecules, such as amino acids,⁹¹ vitamins,^{56,92} lactate,⁹³ dopamine (DA),^{30,94,95} choline, cholesterol,^{60,96} uric acid (UA),⁹⁷ glucose,^{19,32,98-101} and 3-nitrotyrosine (3-NT),⁵⁹ have already been detected by using ECL-POCT devices. Some devices are also designed to achieve high throughput analysis.^{22,33,58,102} Among various molecules, glucose has been intensively studied because it is the main energy substance and can be easily detected, followed by dopamine and choline. The advantage of a POCT device is that it can detect these small molecules anytime, anywhere, so as to monitor personal health.

Because various small molecules can indicate the health level, high throughput analysis is particularly attractive. Sojic *et al.*³³ have developed an ECL sensor based on wireless bipolar electrodes (BPE) to detect glucose and choline simultaneously (Fig. 5A). The quantitative analysis of two analytes was achieved by exploiting the intrinsic enzymatic selectivity, namely, the detection of glucose with a $[\text{Ru}(\text{bpy})_3]^{2+}/\text{GDH}$ system and that of choline with luminol/

ChOx. Because the reactions at both poles of BPE occur in the same solution, the electroactive compounds may react with electrogenerated coreactant intermediates and thus inhibit the ECL emission. To avoid this problem, the Wang group reported an ECL sensing platform based on a multichannel closed bipolar electrode system for detecting H_2O_2 , ascorbic acid (AA), glucose, tripropylamine (TPA), and blood sugar. This design exhibited similar properties to those of a keypad lock. Using the correct order of introduced inputs and increasing the driving voltage can provide a visible ECL signal.²² Multicomponent assays and cross-reactivity were both satisfied for analysis. Moreover, Xu *et al.* developed a SEES for detecting H_2O_2 , glucose, and uric acid (Fig. 5B).⁵⁸ The device is simple, cheap and versatile. Multicomponent analysis can save time and provide repeated data to demonstrate data reliability. Our group has developed a biosensor array with a wheel-like pattern for glucose, lactate, and choline.¹⁰² The biosensor array was constructed by integrating a patterned ITO glass plate with PDMS covers. The separated electrochemical micro-cells enabled simultaneous assay of multiple analytes or samples.

Highly integrated ECL-POCT devices have also been developed to meet the demand of portability and automation in recent years. For instance, Chen *et al.*⁵⁹ fabricated a highly

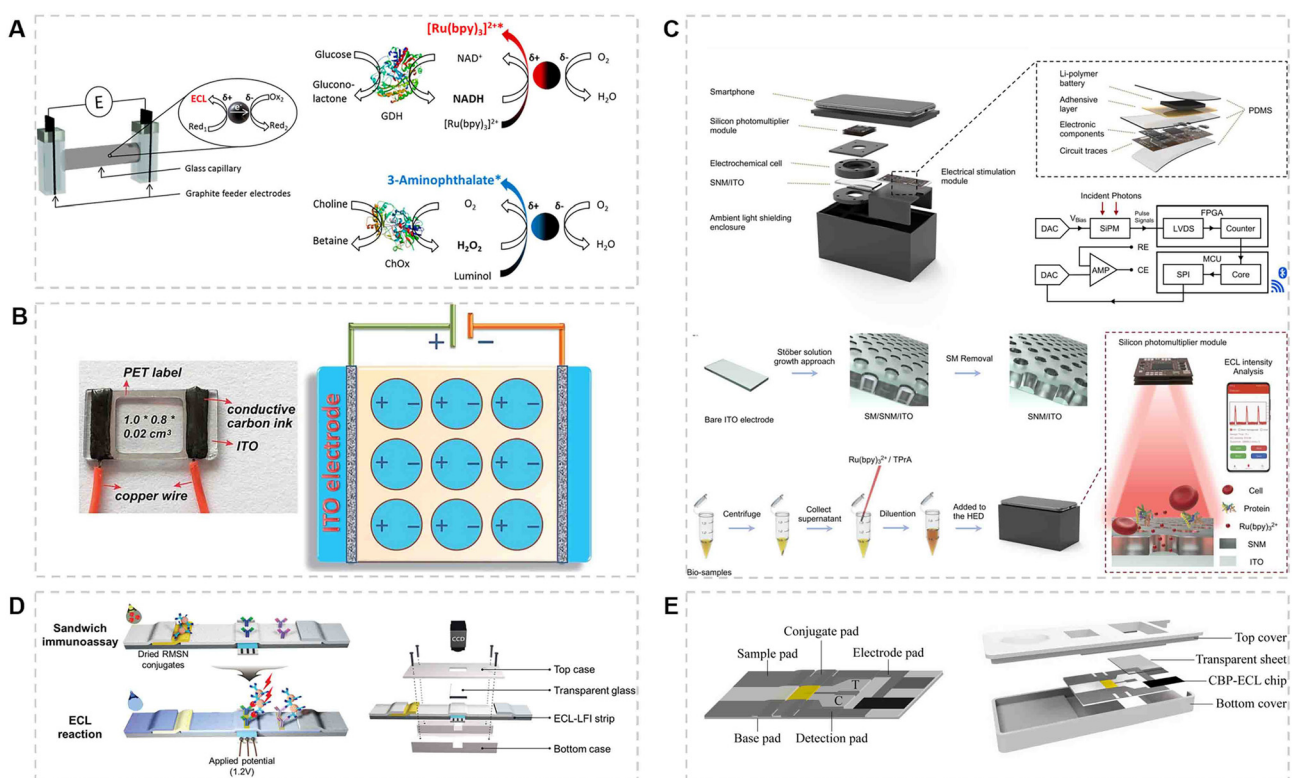


Fig. 5 (A) ECL sensor based on wireless bipolar electrodes (BPE) and suspended carbon microbeads for the detection of glucose and choline simultaneously.³³ Copyright 2016, American Chemical Society. (B) An image of the SEES and a schematic diagram of the SEES with nine micro-electrochemical cells from the top view.⁵⁸ Copyright 2018, Royal Society of Chemistry. (C) Structure, principle and operation process of the handheld ECL analysis device (HED).³⁰ Copyright 2022, Elsevier. (D) Schematic illustration of the ECL-LFS for immunoassay and the structure of the strip device.³⁸ Copyright 2020, Wiley-VCH Verlag. (E) Closed bipolar electrode-ECL (CBP-ECL) immunosensor consisting of a fiber material-based chip and an outer shell for the detection of cTnI.³⁹ Copyright 2022, Elsevier.



integrated handheld ECL analysis device (HED) for the detection of DA (Fig. 5C). The device consists of an ITO glass modified with a silicon nanochannel membrane (SNM), a flexible printed circuit board for electrical stimulation and a silicon photomultiplier for optical signal readout. The SNM allows the electrode to analyze complex biological samples such as urine and rat brain homogenates because of its anti-contamination properties. Besides, Wachsmann-Hogiu *et al.*⁹⁷ also developed a device based on a single electrode system for UA, integrating it with a complementary metal-oxide-semiconductor (CMOS) and a touchscreen liquid crystal display (LCD). Sample handling and data collection can be accomplished on the same platform. It is worth mentioning that a highly integrated device has an extremely simple operating procedure, which enables POCT without specialized training.

4.4 Diagnosis and monitoring of acute diseases

Acute myocardial infarction (AMI) is generally considered to be intractable, because it is asymptomatic, rapid, and fatal. It has the highest proportion of mortality and morbidity among cardiovascular diseases worldwide. Cardiac troponin I (cTnI) is a standard biomarker for both the early diagnosis of AMI and postoperative continuous monitoring, due to its characteristics of early appearance, slow disappearance, and a long diagnostic window period,³⁸ but its basal level in serum is less than 0.1 ng mL^{-1} .^{103,104} In addition to cTnI, the highly sensitive C-reaction protein (hs-CRP) with a concentration of $\mu\text{g mL}^{-1}$ has been found to be a novel marker for AMI.¹⁰⁵ During stroke and myocardial infarction, CRP is elevated with concentrations ranging from 1 to $500 \mu\text{g mL}^{-1}$. Therefore, full-range CRP testing is essential to identify patients who require close follow-up or intensive treatment after a heart attack.³⁷

Kim *et al.*³⁸ have reported an ECL-based LFS to detect cTnI in human serum with a short test time (Fig. 5D). The electrode was attached to the strip using a cover plate. Ru(bpy)₃²⁺-loaded mesoporous silica nanoparticles (RMSNs) were used as probes, which improved the detection sensitivity by three orders of magnitude compared with traditional fluorescence detection. In another work of this group, the probe in the ECL-LFS was replaced with Ru(bpy)₃²⁺-labeled gold nanoparticles, achieving full-range detection of serum CRP with a detection limit of 4.6 pg mL^{-1} within 15 min.³⁷ These studies demonstrate that the ECL-LFS shows high precision and good linearity in the detection of real samples. In order to further improve the sensitivity, Zhang *et al.*³⁹ used a cloth with a screen-printed electrode as the reaction membrane in a CBP-ECL immunosensor (Fig. 5E). Meanwhile, Ru(II)-L-Cys, as a self-enhanced ECL probe, was introduced into the immunosensor, which promoted the generation of much stronger ECL signals and avoided the cumbersome procedures for addition of extra-molecular co-reactants and the influence of the microenvironment. This immunosensor gave rise to a detection sensitivity toward

cTnI as low as $0.4416 \text{ pg mL}^{-1}$. Compared with traditional LFS, such sensing platforms significantly improved the detection sensitivity. Upon further integrating with mobile devices, such as smartphones, paper-based ECL-POCT is expected to be widely used in the future.

5. Conclusions and future perspectives

Ease of control, high reliability and sensitivity, high throughput, real-time analysis and low sample volume requirements make ECL-POCT devices particularly attractive. More recently, the performance of ECL-POCT devices have been greatly improved, thanks to the development of fabrication techniques, miniaturized and portable platforms, and detection mechanisms. Therefore, ECL-POCT devices have been widely used for immunoassay, food and environment monitoring, bioanalysis, clinical diagnostics, and many other purposes. However, to further promote the real applications of ECL-POCT devices, it is necessary to conduct multidisciplinary research to realize their full portability, de-laboratory, de-specialization and automation.

First, it is not hard to see that most research studies are devoted to the development of new materials to modify the electrode or new strategies to amplify the signal to improve the sensitivity of ECL-POCT devices. One of additional key issues is how to improve the antifouling ability of the electrode in complex samples. In the case of ECL-LPS devices, the other one is how to fabricate the electrode directly on the cellulose paper substrate and meanwhile maintain the capillary flow of liquid samples. Second, a micro-electrochemical system that consists of electrochemical stimulation, signal record and transmission, and data analysis units is needed to realize the full portability of ECL-POCT devices. Wireless control *via* Bluetooth or near field communication is definitely the preferential choice. Indeed, there is a continuous effort being made to exploit smartphones or intelligent devices with a wireless control function for ECL-POCT. For instance, smartphones can power devices, capture ECL signals and analyze them through a specific app to automatically give the desired results. Last but not least, a smart combination of different techniques and elements to fabricate fully integrated, miniaturized, automated and multi-functional devices is still challenging and remains to be the direction of future research.

Author contributions

X. Ying wrote the draft of the manuscript. W. Fu, Y. Wang, L. Zhou and B. Su critically reviewed the manuscript and gave their inputs to improve the manuscript. All the authors thoroughly read the final manuscript draft and gave permission for its submission.



Conflicts of interest

The authors declare no conflict of interest.

Acknowledgements

This work was supported by the National Natural Science Foundation of China (22125405 and 22074131).

References

- Y. Zhang and N. Zhou, *Electroanalysis*, 2021, **34**, 168–183.
- P. Bertoncello, A. J. Stewart and L. Dennany, *Anal. Bioanal. Chem.*, 2014, **406**, 5573–5587.
- W. Miao, *Chem. Rev.*, 2008, **108**, 2506–2553.
- S. Deng and H. Ju, *Analyst*, 2013, **138**, 43–61.
- S. Jain, M. Nehra, R. Kumar, N. Dilbaghi, T. Hu, S. Kumar, A. Kaushik and C. Z. Li, *Biosens. Bioelectron.*, 2021, **179**, 113074.
- X. Wang, Y. Luo, K. Huang and N. Cheng, *Advanced Agrochem*, 2022, **1**, 3–6.
- Z. Zhang, P. Ma, R. Ahmed, J. Wang, D. Akin, F. Soto, B. F. Liu, P. Li and U. Demirci, *Adv. Mater.*, 2022, **34**, 2103646.
- M. Xiao, F. Tian, X. Liu, Q. Zhou, J. Pan, Z. Luo, M. Yang and C. Yi, *Adv. Sci.*, 2022, **9**, 2105904.
- Y. Li, S. Man, S. Ye, G. Liu and L. Ma, *Compr. Rev. Food Sci. Food Saf.*, 2022, **21**, 3770–3798.
- R. Liu, A. Fu, Z. Deng, Y. Li and T. Liu, *View*, 2020, **1**, e4.
- S. Xia, J. Pan, D. Dai, Z. Dai, M. Yang and C. Yi, *Chin. Chem. Lett.*, 2022, 107799, DOI: [10.1016/j.cclet.2022.107799](https://doi.org/10.1016/j.cclet.2022.107799).
- Y. Hang, J. Boryczka and N. Wu, *Chem. Soc. Rev.*, 2022, **51**, 329–375.
- S. Shrivastava, T. Q. Trung and N. E. Lee, *Chem. Soc. Rev.*, 2020, **49**, 1812–1866.
- G. Chen, X. Xiao, X. Zhao, T. Tat, M. Bick and J. Chen, *Chem. Rev.*, 2022, **122**, 3259–3291.
- M. Zarei, *Biosens. Bioelectron.*, 2017, **98**, 494–506.
- M. Bhaiyya, P. K. Pattnaik and S. Goel, *Curr. Opin. Electrochem.*, 2021, **30**, 100800.
- A. Roda, M. Mirasoli, E. Michelini, M. Di Fusco, M. Zangheri, L. Cevenini, B. Roda and P. Simoni, *Biosens. Bioelectron.*, 2016, **76**, 164–179.
- C. Parolo, A. Sena-Torralba, J. F. Bergua, E. Calucho, C. Fuentes-Chust, L. Hu, L. Rivas, R. Alvarez-Diduk, E. P. Nguyen, S. Cinti, D. Quesada-Gonzalez and A. Merkoci, *Nat. Protoc.*, 2020, **15**, 3788–3816.
- L. Chen, C. Zhang and D. Xing, *Sens. Actuators, B*, 2016, **237**, 308–317.
- S. Wang, L. Ge, M. Yan, J. Yu, X. Song, S. Ge and J. Huang, *Sens. Actuators, B*, 2013, **176**, 1–8.
- Y. Zhang, J. Xu, S. Zhou, L. Zhu, X. Lv, J. Zhang, L. Zhang, P. Zhu and J. Yu, *Anal. Chem.*, 2020, **92**, 3874–3881.
- X. Zhang, J. Li, X. Jia, D. Li and E. Wang, *Anal. Chem.*, 2014, **86**, 5595–5599.
- K. Kadimisetty, S. Malla and J. F. Rusling, *ACS Sens.*, 2017, **2**, 670–678.
- W. Guo, Y. Liu, Z. Cao and B. Su, *J. Anal. Test.*, 2017, **1**, 14.
- S. R. Chinnadayyala, J. Park, L. Hien Thi Ngoc, M. Santhosh, A. N. Kadam and S. Cho, *Biosens. Bioelectron.*, 2019, **126**, 68–81.
- C. Meng, S. Knežević, F. Du, Y. Guan, F. Kanoufi, N. Sojic and G. Xu, *eScience*, 2022, **2**, 591–605.
- J. Shen, Y. Li, H. Gu, F. Xia and X. Zuo, *Chem. Rev.*, 2014, **114**, 7631–7677.
- H. Torul, M. Durak, I. H. Boyaci and U. Tamer, *Electrochim. Acta*, 2022, **426**, 140769.
- M. L. Bhaiyya, P. K. Pattnaik and S. Goel, *IEEE Trans. Instrum. Meas.*, 2021, **70**, 1–8.
- L. Zhu, W. Fu, J. Chen, S. Li, X. Xie, Z. Zhang, J. Liu, L. Zhou, B. Su and X. Chen, *Sens. Actuators, B*, 2022, **366**, 131972.
- X. Liu, L. Shi, H. Li, W. Niu and G. Xu, *Electrochim. Commun.*, 2007, **9**, 2666–2670.
- M. Sentic, S. Arbault, B. Goudeau, D. Manojlovic, A. Kuhn, L. Bouffier and N. Sojic, *Chem. Commun.*, 2014, **50**, 10202–10205.
- A. de Pouliquen, B. Diez-Buitrago, M. Dumont Milutinovic, M. Sentic, S. Arbault, L. Bouffier, A. Kuhn and N. Sojic, *Anal. Chem.*, 2016, **88**, 6585–6592.
- W. Gao, M. Saqib, L. Qi, W. Zhang and G. Xu, *Curr. Opin. Electrochem.*, 2017, **3**, 4–10.
- E. B. Bahadir and M. K. Sezgintürk, *TrAC, Trends Anal. Chem.*, 2016, **82**, 286–306.
- V. T. Nguyen, S. Song, S. Park and C. Joo, *Biosens. Bioelectron.*, 2020, **152**, 112015.
- D. Hong, K. Kim, E. J. Jo and M. G. Kim, *Anal. Chem.*, 2021, **93**, 7925–7932.
- D. Hong, E. J. Jo, K. Kim, M. B. Song and M. G. Kim, *Small*, 2020, **16**, 2004535.
- T. Zhan, Y. Su, W. Lai, Z. Chen and C. Zhang, *Biosens. Bioelectron.*, 2022, **214**, 114494.
- M. Liu, S. Suo, J. Wu, Y. Gan, D. Ah Hanaor and C. Q. Chen, *J. Colloid Interface Sci.*, 2019, **539**, 379–387.
- L. Fu and Y. Wang, *TrAC, Trends Anal. Chem.*, 2018, **107**, 196–211.
- E. M. Gross, H. E. Durant, K. N. Hipp and R. Y. Lai, *ChemElectroChem*, 2017, **4**, 1594–1603.
- Y. Xia, J. Si and Z. Li, *Biosens. Bioelectron.*, 2016, **77**, 774–789.
- K. Kadimisetty, I. M. Mosa, S. Malla, J. E. Satterwhite-Warden, T. M. Kuhns, R. C. Faria, N. H. Lee and J. F. Rusling, *Biosens. Bioelectron.*, 2016, **77**, 188–193.
- J. Zhao, C. Chen, J. Zhu, H. Zong, Y. Hu and Y. Wang, *Anal. Chem.*, 2022, **94**, 4303–4310.
- W. Luo, H. Chu, X. Wu, P. Ma, Q. Wu and D. Song, *Talanta*, 2022, **239**, 123083.
- L. Ge, J. Yan, X. Song, M. Yan, S. Ge and J. Yu, *Biomaterials*, 2012, **33**, 1024–1031.
- L. Li, W. Li, C. Ma, H. Yang, S. Ge and J. Yu, *Sens. Actuators, B*, 2014, **202**, 314–322.
- L. Wu, C. Ma, L. Ge, Q. Kong, M. Yan, S. Ge and J. Yu, *Biosens. Bioelectron.*, 2015, **63**, 450–457.



50 H. Liu, X. Zhou, W. Liu, X. Yang and D. Xing, *Anal. Chem.*, 2016, **88**, 10191–10197.

51 V. Mani, K. Kadimisetty, S. Malla, A. A. Joshi and J. F. Rusling, *Environ. Sci. Technol.*, 2013, **47**, 1937–1944.

52 P. Nikolaou, E. L. Sciuto, A. Zanut, S. Petralia, G. Valenti, F. Paolucci, L. Prodi and S. Conoci, *Biosens. Bioelectron.*, 2022, **209**, 114165.

53 Y. Katayama, T. Ohgi, Y. Mitoma, E. Hifumi and N. Egashira, *Anal. Bioanal. Chem.*, 2016, **408**, 5963–5971.

54 S. Li, J. Liu, Z. Chen, Y. Lu, S. S. Low, L. Zhu, C. Cheng, Y. He, Q. Chen, B. Su and Q. Liu, *Sens. Actuators, B*, 2019, **297**, 126811.

55 M. Bhaiyya, M. B. Kulkarni, P. K. Pattnaik and S. Goel, *Luminescence*, 2022, **37**, 357–365.

56 M. Bhaiyya, P. K. Pattnaik and S. Goel, *Microfluid. Nanofluid.*, 2021, **25**, 41.

57 I. Bist, B. Song, I. M. Mosa, T. E. Keyes, A. Martin, R. J. Forster and J. F. Rusling, *ACS Sens.*, 2016, **1**, 272–278.

58 W. Gao, K. Muzyka, X. Ma, B. Lou and G. Xu, *Chem. Sci.*, 2018, **9**, 3911–3916.

59 L. Zhu, S. Li, W. Liu, J. Chen, Q. Yu, Z. Zhang, Y. Li, J. Liu and X. Chen, *Biosens. Bioelectron.*, 2021, **187**, 113284.

60 D. Wang, C. Liu, Y. Liang, Y. Su, Q. Shang and C. Zhang, *J. Electrochem. Soc.*, 2018, **165**, B361–B369.

61 L. D'Alton, S. Carrara, G. J. Barbante, D. Hoxley, D. J. Hayne, P. S. Francis and C. F. Hogan, *Bioelectrochemistry*, 2022, **146**, 108107.

62 F. Du, Z. Dong, Y. Guan, A. M. Zeid, D. Ma, J. Feng, D. Yang and G. Xu, *Anal. Chem.*, 2022, **94**, 2189–2194.

63 T. Liu, J. He, Z. Lu, M. Sun, M. Wu, X. Wang, Y. Jiang, P. Zou, H. Rao and Y. Wang, *Chem. Eng. J.*, 2022, **429**, 132462.

64 Y. Zhang, Y. Cui, M. Sun, T. Wang, T. Liu, X. Dai, P. Zou, Y. Zhao, X. Wang, Y. Wang, M. Zhou, G. Su, C. Wu, H. Yin, H. Rao and Z. Lu, *Biosens. Bioelectron.*, 2022, **209**, 114262.

65 S. Li, D. Zhang, J. Liu, C. Cheng, L. Zhu, C. Li, Y. Lu, S. S. Low, B. Su and Q. Liu, *Biosens. Bioelectron.*, 2019, **129**, 284–291.

66 S. Liu, C. Gao, Z. Tong, X. Mu, B. Liu, J. Xu, B. Du, J. Wang and Z. Liu, *Anal. Bioanal. Chem.*, 2022, **414**, 1095–1104.

67 H. Liu, X. Zhou, Q. Shen and D. Xing, *Theranostics*, 2018, **8**, 2289–2299.

68 R. Svilgelj, I. Zuliani, N. Dossi and R. Toniolo, *Anal. Bioanal. Chem.*, 2022, **414**, 7935–7941.

69 W. Li, L. Li, S. Ge, X. Song, L. Ge, M. Yan and J. Yu, *Chem. Commun.*, 2013, **49**, 7687–7689.

70 J. Yan, L. Ge, X. Song, M. Yan, S. Ge and J. Yu, *Chemistry*, 2012, **18**, 4938–4945.

71 J. Yan, M. Yan, L. Ge, S. Ge and J. Yu, *Sens. Actuators, B*, 2014, **193**, 247–254.

72 W. Li, L. Li, S. Li, X. Wang, M. Li, S. Wang and J. Yu, *Sens. Actuators, B*, 2013, **188**, 417–424.

73 L. Li, Y. Zhang, L. Zhang, S. Ge, H. Liu, N. Ren, M. Yan and J. Yu, *Anal. Chem.*, 2016, **88**, 5369–5377.

74 H. Yang, Y. Zhang, L. Li, L. Zhang, F. Lan and J. Yu, *Anal. Chem.*, 2017, **89**, 7511–7519.

75 L. Wu, Y. Zhang, Y. Wang, S. Ge, H. Liu, M. Yan and J. Yu, *Microchim. Acta*, 2016, **183**, 1873–1880.

76 S. Ge, J. Zhao, S. Wang, F. Lan, M. Yan and J. Yu, *Biosens. Bioelectron.*, 2018, **102**, 411–417.

77 H. W. Shi, M. S. Wu, Y. Du, J. J. Xu and H. Y. Chen, *Biosens. Bioelectron.*, 2014, **55**, 459–463.

78 L. Li, Y. Zhang, F. Liu, M. Su, L. Liang, S. Ge and J. Yu, *Chem. Commun.*, 2015, **51**, 14030–14033.

79 Y. Chen, J. Wang, Z. Liu, X. Wang, X. Li and G. Shan, *Biochem. Eng. J.*, 2018, **129**, 1–6.

80 Q. Feng, H. Chen and J. Xu, *Sci. China: Chem.*, 2015, **58**, 810–818.

81 Y. Zhang and D. Ding, *View*, 2022, **3**, 20200138.

82 H. Torul, E. Çalkı Kayış, I. H. Boyaci and U. Tamer, *Analyst*, 2022, **147**, 4866–4875.

83 Z. Li, M. You, Y. Bai, Y. Gong and F. Xu, *Small Methods*, 2020, **4**, 1900459.

84 D. Jiang, L. Zhang, F. Liu, C. Liu, L. Liu and X. Pu, *RSC Adv.*, 2016, **6**, 19676–19685.

85 J. Jang, H. G. Hur, M. J. Sadowsky, M. N. Byappanahalli, T. Yan and S. Ishii, *J. Appl. Microbiol.*, 2017, **123**, 570–581.

86 J. D. van Elsas, A. V. Semenov, R. Costa and J. T. Trevors, *ISME J.*, 2011, **5**, 173–183.

87 M. Liu, R. Liu, D. Wang, C. Liu and C. Zhang, *Lab Chip*, 2016, **16**, 2860–2870.

88 M. Liu, D. Wang, C. L. Liu, R. Liu, H. J. Li and C. S. Zhang, *Sens. Actuators, B*, 2017, **246**, 327–335.

89 J. M. Farber and P. I. Peterkin, *Microbiol. Rev.*, 1991, **55**, 476–511.

90 U. Gasanov, D. Hughes and P. M. Hansbro, *FEMS Microbiol. Rev.*, 2005, **29**, 851–875.

91 L. Ge, S. Wang, S. Ge, J. Yu, M. Yan, N. Li and J. Huang, *Chem. Commun.*, 2014, **50**, 5699–5702.

92 M. Bhaiyya, P. K. Pattnaik and S. Goel, *Sens. Actuators, A*, 2021, **331**, 112831.

93 Y. Yao, H. Li, D. Wang, C. Liu and C. Zhang, *Analyst*, 2017, **142**, 3715–3724.

94 H. J. Kwon, E. C. Rivera, M. R. C. Neto, D. Marsh, J. J. Swerdlow, R. L. Summerscales and P. P. Tadi Uppala, *Results Chem.*, 2020, **2**, 100029.

95 X. Zhang, C. Chen, J. Li, L. Zhang and E. Wang, *Anal. Chem.*, 2013, **85**, 5335–5339.

96 M. A. Carvajal, J. Ballesta-Claver, D. P. Morales, A. J. Palma, M. C. Valencia-Miron and L. F. Capitan-Vallvey, *Sens. Actuators, B*, 2012, **169**, 46–53.

97 R. Abbasi, J. Liu, S. Suarasan and S. Wachsmann-Hogiu, *Lab Chip*, 2022, **22**, 994–1005.

98 X. Zhang, J. Li, C. Chen, B. Lou, L. Zhang and E. Wang, *Chem. Commun.*, 2013, **49**, 3866–3868.

99 M. Salve, A. Mandal, K. Amreen, B. V. V. S. N. P. Rao, P. K. Pattnaik and S. Goel, *IEEE Trans. Instrum. Meas.*, 2021, **70**, 9501710.

100 W. Guan, M. Liu and C. Zhang, *Biosens. Bioelectron.*, 2016, **75**, 247–253.

101 M. Bhaiyya, P. Rewatkar, M. Salve, P. K. Pattnaik and S. Goel, *IEEE Trans. Nanobioscience*, 2021, **20**, 79–85.



102 Z. Zhou, L. Xu, S. Wu and B. Su, *Analyst*, 2014, **139**, 4934–4939.

103 Z. Yang and D. Min Zhou, *Clin. Biochem.*, 2006, **39**, 771–780.

104 Q. Wu, Y. Sun, D. Zhang, S. Li, Y. Zhang, P. Ma, Y. Yu, X. Wang and D. Song, *Biosens. Bioelectron.*, 2017, **96**, 288–293.

105 C. Statescu, L. Anghel, B. S. Tudurachi, A. Leonte, L. C. Benchea and R. A. Sascau, *Int. J. Mol. Sci.*, 2022, **23**, 9168.

